

Permutation-Aware Action Segmentation via Unsupervised Frame-to-Segment Alignment

Quoc-Huy Tran*

Ahmed Mehmood*

Muhammad Ahmed

Muhammad Naufil

Anas Zafar

Andrey Konin

M. Zeeshan Zia

Retrocausal, Inc.

Redmond, WA

www.retrocausal.ai

Abstract

This paper presents a novel transformer-based framework for unsupervised activity segmentation which leverages not only frame-level cues but also segment-level cues. This is in contrast with previous methods which often rely on frame-level information only. Our approach begins with a frame-level prediction module which estimates framewise action classes via a transformer encoder. The frame-level prediction module is trained in an unsupervised manner via temporal optimal transport. To exploit segment-level information, we introduce a segment-level prediction module and a frame-to-segment alignment module. The former includes a transformer decoder for estimating video transcripts, while the latter matches frame-level features with segment-level features, yielding permutation-aware segmentation results. Moreover, inspired by temporal optimal transport, we develop simple-yet-effective pseudo labels for unsupervised training of the above modules. Our experiments on four public datasets, i.e., 50 Salads, YouTube Instructions, Breakfast, and Desktop Assembly show that our approach achieves comparable or better performance than previous methods in unsupervised activity segmentation.

1. Introduction

Temporal activity segmentation [17, 43, 8, 40, 50, 5, 61, 34, 11] aims to associate each frame in a video capturing a human activity with one of the action/sub-activity classes. Temporally segmenting human activities in videos plays an important role in several computer vision, robotics, health-care, manufacturing, and surveillance applications. Examples include visual analytics [2, 25, 24, 21] (i.e., compute time and motion statistics such as average cycle time from

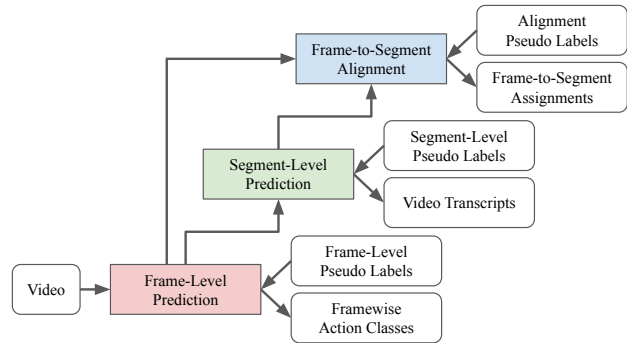


Figure 1: Prior works often utilize only frame-level cues via frame-level prediction modules (i.e., red) to predict framewise action classes. We propose segment-level prediction and frame-to-segment alignment modules (i.e., green and blue), which exploits segment-level cues for permutation-aware segmentation results. Also, we introduce simple-yet-effective pseudo labels for unsupervised training.

video recordings), ergonomics risk assessment [48, 47] (i.e., segment actions of interest in videos for analyzing ergonomics risks), and task guidance [19, 7, 45, 29] (i.e., offer instructions to workers based on expert demonstration videos).

Considerable efforts have been made in designing fully-supervised methods [35, 12, 37, 17, 43] or weakly-supervised methods [32, 51, 53, 13, 8, 40, 44, 58, 27, 50, 5] for temporal activity segmentation due to their great performance. However, acquiring dense framewise labels or weak annotations such as transcripts [32] and timestamps [44] is generally hard and expensive especially for a large number of videos [33, 27]. Therefore, we are interested in unsupervised approaches for temporal activity segmentation, which simultaneously extract actions and segment all video frames into clusters with each cluster representing one ac-

* indicates joint first author

{huy,ahmedraza,ahmed,naufil,anas,andrey,zeeshan}@retrocausal.ai

tion. Early unsupervised methods [56, 33, 65, 42, 68] separate representation learning from clustering, preventing effective feedback between them, while using offline clustering, resulting in memory inefficiency. To address that, UDE [61] and TOT [34] develop joint representation learning and online clustering approaches. The above methods often leverage frame-level information only (i.e., red block in Fig. 1), while not explicitly utilizing high-level information such as transcript, which is crucial for handling permutations of actions, missing actions, and repetitive actions.

In this work, we present a novel unsupervised activity segmentation approach which is based on transformers [64] and exploits both frame-level cues and segment-level cues. Motivated by the strong performance of transformer-based architectures [14, 5] in supervised activity segmentation, our unsupervised model includes a transformer encoder and a transformer decoder. The former performs self-attention to learn dependencies within the video sequence, while the latter relies on cross-attention to learn dependencies between the video sequence and the transcript sequence, resulting in effective contextual features. In addition to the frame-level prediction module for exploiting frame-level cues, we add a segment-level prediction module and a frame-to-segment alignment module (i.e., green and blue blocks in Fig. 1) to leverage segment-level cues, yielding permutation-aware segmentation results. For unsupervised training of the above modules, we propose simple-yet-effective pseudo labels based on temporal optimal transport [34]. We demonstrate comparable or superior performance of our approach over previous unsupervised activity segmentation methods on four public datasets.

In summary, our contributions include:

- We propose a novel transformer-based approach for unsupervised activity segmentation. In addition to using frame-level cues, we add both a segment-level prediction module and a frame-to-segment alignment module to exploit segment-level cues, leading to permutation-aware segmentation results.
- We introduce simple-yet-effective pseudo labels based on temporal optimal transport, enabling unsupervised training of the segment-level prediction module and the frame-to-segment alignment module.
- Extensive evaluations on 50 Salads, YouTube Instructions, Breakfast, and Desktop Assembly datasets show that our approach performs on par with or better than prior methods in unsupervised activity segmentation.

2. Related Work

Fully-Supervised Activity Segmentation. Early works in fully-supervised activity segmentation often rely on sliding temporal window with non-maximum suppression [54, 26]

or structured temporal modeling via hidden Markov models [62, 31], while recent methods are mostly based on temporal convolutional networks (TCNs) [35, 12, 37, 17, 43]. Lea et al. [35] develop the first TCN-based solution, which includes an encoder-decoder architecture with temporal convolutions and deconvolutions to capture long-range temporal dependencies. TricorNet [12] replaces the above decoder by a bi-directional LSTM, while TDRN [37] employs deformable temporal convolutions instead. Since these methods downsample videos to a temporal resolution, they fail to capture fine-grained details. Thus, multi-stage TCNs [17, 43] are introduced to maintain a high temporal resolution. However, due to performing framewise prediction, the above methods suffer from over-segmentation. To address that, refinement techniques, e.g., graph-based reasoning [22] and boundary detection [23], are proposed.

Weakly-Supervised Activity Segmentation. Weakly-supervised activity segmentation methods utilize different forms of weak labels, including the ordered list of actions appearing in the video, i.e., transcript supervision [32, 51, 53, 13, 8, 40], or the set of actions occurring in the video, i.e., set supervision [52, 18, 41]. Recently, timestamp supervision [44, 58, 27, 50], which requires labeling a single frame per action segment, has attracted research interests, since it has similar annotation costs as transcript supervision but it yields better results thanks to the additional approximate segment location information in timestamp labels. More recently, Behrmann et al. [5] introduce a unified fully-supervised and timestamp-supervised method, achieving competitive results. The aforementioned methods need either framewise labels for full supervision or weak labels for weak supervision, whereas our approach does not.

Unsupervised Activity Segmentation. Early attempts [57, 3] in unsupervised activity segmentation often utilize the narrations accompanied with the videos, however, these narrations are not always provided. That motivates the development of methods with only visual inputs [56, 33, 65, 42, 61, 68, 34]. Mallow [56] learns an appearance model and a temporal model of the activity in an alternating manner. CTE [33] first learns a temporal embedding and then clusters the embedded features with K-means. To improve CTE, VTE [65] adds a visual embedding, while ASAL [42] adds an action-level embedding. SSCAP [68] first uses a video-based self-supervised model for feature extraction and then performs co-occurrence action parsing to capture the temporal structure of the activity. These methods separate representation learning from offline clustering. Recently, UDE [61] and TOT [34] perform joint representation learning and online clustering. Unlike the above methods, which often exploit frame-level cues only, we propose modules for exploiting segment-level cues as well as pseudo labels for unsupervised training, yielding improved results.

Transformers in Activity Segmentation. After the suc-

Successful application of transformers [64] in natural language processing, there has been a wide adoption of transformers in computer vision tasks [14, 9, 4, 6]. Transformers focus on the attention mechanism to extract contextual information over the entire sequence. Recently, a few methods [69, 5] have applied transformers for temporal activity segmentation. ASFormer [69] consists of a few encoder blocks, each of which includes a dilated temporal convolution and a self-attention layer, and decoder blocks, where cross-attention is used to gather information from encoder blocks. Due to making framewise prediction, ASFormer suffers from over-segmentation. To address that, UVAST [5] uses a transformer decoder to predict the transcript and exploit segment-level cues. Although we adopt the transformer encoder of ASFormer and the transformer decoder of UVAST, our overall architecture is different from both. Also, they both require labels for supervised training, whereas we introduce pseudo labels for unsupervised training.

3. Our Approach

We present below our main contribution, an unsupervised transformer-based approach for temporal activity segmentation. Fig. 2 shows an overview of our approach.

Notations. Let us first represent the encoder function and the decoder function as f_θ and g_ϕ respectively (with learnable parameters θ and ϕ). Our approach takes as input a sequence of B frames, represented as $\mathbf{X} = [\mathbf{x}_1, \mathbf{x}_2, \dots, \mathbf{x}_B]^\top$. The encoder features of \mathbf{X} are expressed as $\mathbf{E} = [e_1, e_2, \dots, e_B]^\top \in \mathbb{R}^{B \times d}$ with $e_i = f_\theta(\mathbf{x}_i) \in \mathbb{R}^d$ (d is the feature dimension). Next, let us denote $\mathbf{A} = [1, 2, \dots, K]^\top \in \mathbb{R}^K$ as the sequence of K action classes in the activity. Our approach learns a group of K prototypes, represented as $\mathbf{C} = [c_1, c_2, \dots, c_K]^\top \in \mathbb{R}^{K \times d}$ with $c_j \in \mathbb{R}^d$ corresponding to the j -th action class in \mathbf{A} . We denote $\mathbf{T} = [a_1, a_2, \dots, a_N]^\top \in \mathbb{R}^N$ (with $a_j \in \mathbf{A}$) as the transcript which contains the sequence of actions appearing in \mathbf{X} , and $\mathbf{S} \in \mathbb{R}^{N \times d}$ as the transcript features. The decoder features are written as $\mathbf{D} = [d_1, d_2, \dots, d_N]^\top \in \mathbb{R}^{N \times d}$ with $d_j \in \mathbb{R}^d$ corresponding to a_j in \mathbf{T} . Finally, we represent $\mathbf{P}_f \in \mathbb{R}^{B \times K}$, $\mathbf{P}_s \in \mathbb{R}^{N \times K}$, and $\mathbf{P}_a \in \mathbb{R}^{B \times K}$ as the *predicted* assignment probabilities (i.e., predicted ‘‘codes’’) at the frame-level prediction module (i.e., between frames and actions), the segment-level prediction module (i.e., between transcript positions and actions), and the frame-to-segment alignment module (i.e., between frames and actions) respectively. Similarly, $\mathbf{Q}_f \in \mathbb{R}^{B \times K}$, $\mathbf{Q}_s \in \mathbb{R}^{N \times K}$, and $\mathbf{Q}_a \in \mathbb{R}^{B \times K}$ denote the corresponding *pseudo-label* assignment probabilities (i.e., pseudo-label ‘‘codes’’) for \mathbf{P}_f , \mathbf{P}_s , and \mathbf{P}_a respectively.

3.1. Unsupervised Frame-Level Prediction

Here we describe our frame-level prediction module which leverages frame-level cues for unsupervised activity

segmentation. For that purpose, we adopt the joint representation learning and online clustering method proposed in [34]. However, unlike their method, we introduce additional modules in Secs. 3.2 and 3.3 for exploiting segment-level cues. Also, we use the transformer encoder provided in [5] to capture long-range dependencies via self-attention.

The input frames \mathbf{X} are first passed through the transformer encoder f_θ to yield the encoder features \mathbf{E} . The frame-level predicted codes \mathbf{P}_f (with P_f^{ij} denoting the probability that the i -th frame in \mathbf{X} is assigned to the j -th action in \mathbf{A}) are then computed as $\mathbf{P}_f = \text{softmax}\left(\frac{1}{\tau} \mathbf{E} \mathbf{C}^\top\right)$ with a temperature parameter τ . We follow [34] to obtain the frame-level pseudo-label codes \mathbf{Q}_f by solving the below temporal optimal transport problem:

$$\max_{\mathbf{Q} \in \mathcal{Q}} \text{Tr}(\mathbf{Q}^\top \mathbf{E} \mathbf{C}^\top) - \rho \text{KL}(\mathbf{Q} \| \mathbf{M}_A), \quad (1)$$

$$\mathcal{Q} = \left\{ \mathbf{Q} : \mathbf{Q} \mathbf{1}_K = \frac{1}{B} \mathbf{1}_B, \mathbf{Q}^\top \mathbf{1}_B = \frac{1}{K} \mathbf{1}_K \right\}, \quad (2)$$

where ρ is a balancing parameter, and $\mathbf{1}_B$ and $\mathbf{1}_K$ are vectors of ones with B and K dimensions respectively. The first term in Eq. 1 measures the similarity between the features \mathbf{E} and the prototypes \mathbf{C} , while the second term denotes the Kullback-Leibler divergence between \mathbf{Q}_f and the prior distribution \mathbf{M}_A [60]. In particular, \mathbf{M}_A assumes the *fixed order* of actions \mathbf{A} , and enforces initial frames in \mathbf{X} to be assigned to initial actions in \mathbf{A} and subsequent frames in \mathbf{X} to be assigned to subsequent actions in \mathbf{A} . In Sec. 3.2, we will discuss relaxing the above fixed-order prior by introducing the transcript \mathbf{T} and enabling permutations of actions. Eq. 2 represents the *equal partition* constraint, which imposes that each action in \mathbf{A} is assigned the same number of frames in \mathbf{X} to avoid a trivial solution. As mentioned in [34], the method works relatively well for activities with various action lengths since the above equal partition constraint is applied on soft assignments. The solution for the temporal optimal transport problem is:

$$\mathbf{Q}_f = \text{diag}(\mathbf{u}) \exp\left(\frac{\mathbf{E} \mathbf{C}^\top + \rho \log \mathbf{M}_A}{\rho}\right) \text{diag}(\mathbf{v}), \quad (3)$$

where $\mathbf{u} \in \mathbb{R}^B$ and $\mathbf{v} \in \mathbb{R}^K$ are renormalization vectors [10]. Fig. 3 shows an example of \mathbf{M}_A and \mathbf{Q}_f , where the red boxes highlight the fixed order of actions $\{3, 4, 5\}$. We minimize the below cross-entropy loss with respect to θ and \mathbf{C} (note that we do not backpropagate through \mathbf{Q}_f):

$$L_f = -\frac{1}{B} \sum_{i=1}^B \sum_{j=1}^K \mathbf{Q}_f^{ij} \log P_f^{ij}. \quad (4)$$

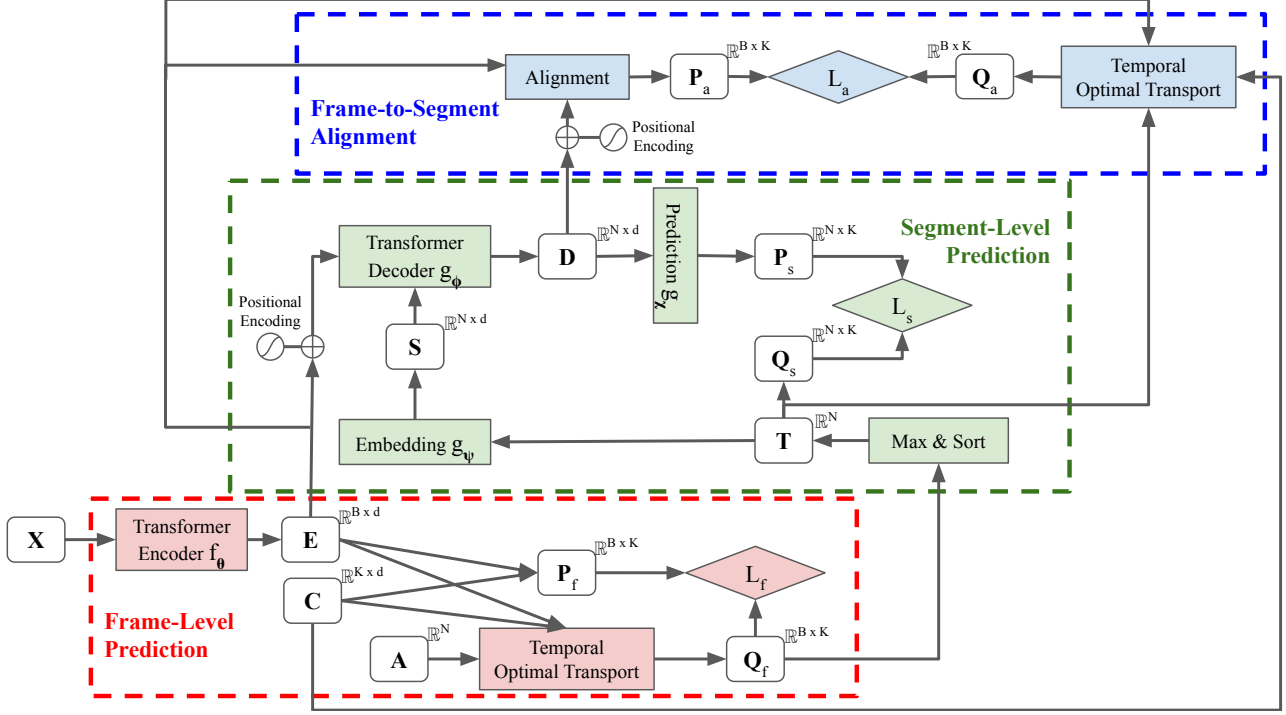


Figure 2: Our approach includes a frame-level prediction module (i.e., red) which extracts frame-level features E via a transformer encoder and uses temporal optimal transport to compute frame-level pseudo labels Q_f for unsupervised training. To exploit segment-level information, we propose a segment-level prediction module (i.e., green), which extract segment-level features D via a transformer decoder, and a frame-to-segment alignment module (i.e., blue), which matches frame-level features E and segment-level features D . In addition, we introduce segment-level pseudo labels Q_s and alignment-level pseudo labels Q_a for unsupervised training of the above modules.

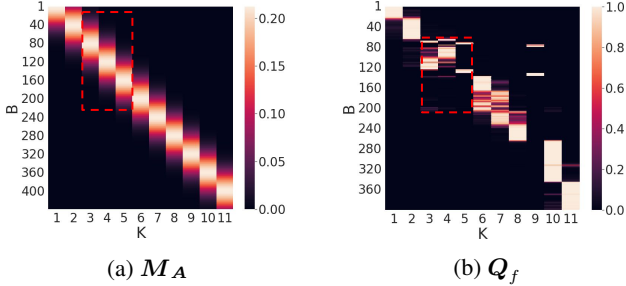


Figure 3: (a) Fixed-order prior distribution M_A . (b) Frame-level pseudo-label codes Q_f .

3.2. Unsupervised Segment-Level Prediction

The above module leverages frame-level cues and the fixed-order prior. In this section, we present our segment-level prediction module to exploit segment-level cues and allow permutations of actions. In particular, we introduce the transcript T , which indicates the sequence of actions of A occurring in the input sequence X . For example, let us assume $A = [1, 2, 3, 4, 5]$, it is possible that $T =$

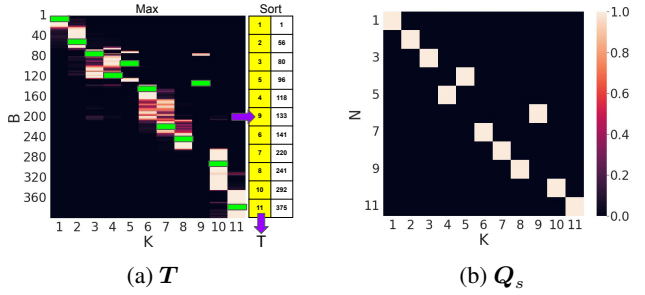


Figure 4: (a) Permutation-aware transcript T . (b) Segment-level pseudo-label codes Q_s .

$[1, 3, 2, 5, 4]$, which is a permutation of A . We will discuss later how T is estimated for unsupervised training.

Assuming the transcript T is given, we first pass it to the embedding layer g_ψ to obtain the transcript features S , which are then fed to the transformer decoder g_ϕ . In addition, we also feed the encoder features E (after positional encoding) to the transformer decoder g_ϕ , which performs cross-attention between E and S to yield the decoder features D . The segment-level predicted codes P_s (with $P_s^{i,j}$

corresponding to the probability that the i -th position in T contains the j -th action in A) are computed by passing the decoder features D to the prediction layer g_χ . In practice, we employ the transformer decoder proposed in [5], which computes P_s in an auto-regressive manner, i.e., a part of T up to the i -th position is used to predict the $(i+1)$ -th row of P_s . In parallel, we convert the transcript T into the segment-level pseudo-label codes Q_s . Specifically, we set $Q_s^{ij} = 1$ if the i -th position in T contains the j -th action in A , and $Q_s^{ij} = 0$ otherwise. We minimize the following cross-entropy loss between P_s and Q_s with respect to θ , ψ , ϕ , and χ (note that we do not backpropagate through Q_s):

$$L_s = -\frac{1}{N} \sum_{i=1}^N \sum_{j=1}^K Q_s^{ij} \log P_s^{ij}. \quad (5)$$

For unsupervised training, we estimate the transcript T from the frame-level pseudo-label codes Q_f . This is in contrast with [5], where framewise labels or timestamp labels are required for supervised training. For each j -th action, we find the i -th frame where Q_f^{ij} has the maximum assignment probability along the j -th column, yielding an action-frame pair (j, i) . Next, we sort all action-frame pairs by their frame indexes. The resulting temporally sorted list of actions is considered as our estimated transcript T . Our motivation is that to predict each action correctly, the method only needs to select a single frame correctly, which is easier than obtaining the correct framewise segmentation result [5]. Fig. 4 illustrates an example of computing T from Q_f , and computing Q_s from T . Note that the above imply that N (the length of the transcript T) is equal to K (the length of the action list A), and our predicted transcript T shares the same set of unique actions with A despite having different orderings. Thus, our method is able to model permutations of actions but not repetitive and missing actions. Similar to [34], our method tends to assign a small number of frames to the missing actions, leading to a slight impact on the overall segmentation accuracy. Handling repetitive actions is an interesting topic and remains our future work.

3.3. Unsupervised Frame-to-Segment Alignment

To further exploit segment-level cues and improve segmentation results, we propose a frame-to-segment alignment module, which matches frame-level features with segment-level features and models permutations of actions. We pass both the encoder features E and the decoder features D (after positional encoding) to the frame-to-segment alignment module, which performs cross-attention between E and D to predict the alignment-level predicted codes P_a . Here, P_a^{ij} corresponds to the probability that the i -th frame in X is mapped to the j -th action in A . Particularly, we compute $P_a = \text{softmax}\left(\frac{1}{\tau'} ED^\top\right)$ with a temperature parameter τ' . Furthermore, to obtain the alignment-level

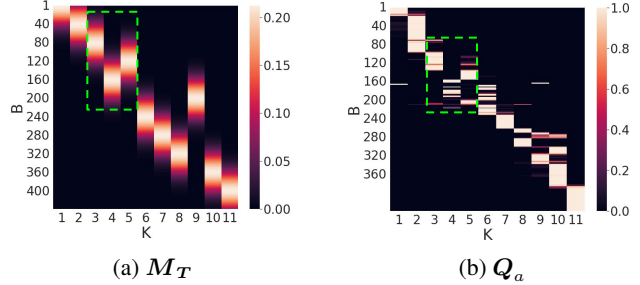


Figure 5: (a) Permutation-aware prior distribution M_T . (b) Alignment-level pseudo-label codes Q_a .

pseudo-label codes Q_a , we propose a modified temporal optimal transport module which is capable of handling permutations of actions. Specifically, instead of using the prior distribution M_A which enforces the fixed order of actions A , we utilize the prior distribution M_T which imposes the permutation-aware transcript T . The solution for the permutation-aware optimal transport problem is:

$$Q_a = \text{diag}(\mathbf{u}) \exp\left(\frac{EC^\top + \rho \log M_T}{\rho}\right) \text{diag}(\mathbf{v}), \quad (6)$$

where $\mathbf{u} \in \mathbb{R}^B$ and $\mathbf{v} \in \mathbb{R}^K$ are renormalization vectors [10]. Fig. 5 shows an example of M_T and Q_a , where the green boxes highlight the permutations of actions $\{3, 5, 4\}$ as compared to the red boxes with the fixed order of actions $\{3, 4, 5\}$ in Fig. 3. As we will show later in Sec. 4.1.2, using the permutation-aware Q_a derived from T yields better performance than using the fixed-order Q_a derived from A . We minimize the cross-entropy loss between P_a and Q_a with respect to θ , ψ , and ϕ (note that we do not backpropagate through Q_a):

$$L_a = -\frac{1}{B} \sum_{i=1}^B \sum_{j=1}^K Q_a^{ij} \log P_a^{ij}. \quad (7)$$

Inspired by deep supervision [36, 38, 39], our final loss for unsupervised training is a combination of the fixed-order loss L_f (Eq. 4) and the permutation-aware losses L_s (Eq. 5) and L_a (Eq. 7):

$$L = L_f + \alpha L_s + \beta L_a, \quad (8)$$

where α and β are the balancing parameters for L_s and L_a respectively. Following [5], we set $\alpha = \beta = 1$.

4. Experiments

Implementation Details. We train our model in two stages. In the first stage, we train only the frame-level prediction module with the loss in Eq. 4 for 30 epochs, which is then

used for initialization in the second stage, where we train the entire model with the loss in Eq. 8 for 70 epochs. Note that we reduce the transformer encoder and transformer decoder proposed in [5] to two layers to avoid overfitting. We implement our approach in pyTorch [49]. We use ADAM optimization [28] with a learning rate of 10^{-3} and a weight decay of 10^{-5} . For inference, we follow [34] to compute cluster assignment probabilities for all frames and then pass them to a Viterbi decoder which smooths out the probabilities given the action order T (instead of A in [34]). More details are provided in the supplementary material.

Competing Methods. We compare our approach, namely *UFSA* (short for *Unsupervised Frame-to-Segment Alignment*), against a narration-based method [3], sequential learning and clustering methods [56, 33, 65, 42, 68], and joint learning and clustering methods [61, 34].

Datasets. We evaluate our approach on four public datasets, i.e., 50 Salads [59], YouTube Instructions (YTI) [3], Breakfast [30], and Desktop Assembly [34]:

- *50 Salads* includes 50 videos capturing 25 actors making 2 types of salads. The total duration of all videos is over 4.5 hours with an average of 10k frames per video. We test on 2 granularity levels, i.e., *Eval* with 12 action classes and *Mid* with 19 action classes. Following [33], we use pre-computed features by [66].
- *YouTube Instructions (YTI)* contains 150 videos capturing 5 activities with 47 action classes in total and an average video length of about 2 minutes. These videos contain many background frames. We use pre-computed features provided by [3].
- *Breakfast* includes 70 hours of videos (30 seconds to a few minutes long per video) capturing 10 cooking activities with 48 action classes in total. We follow [56] to use pre-computed features proposed by [31].
- *Desktop Assembly* contains 2 sets of videos. *Orig* contains 76 videos of 4 actors performing desktop assembly in a fixed order. *Extra* includes all *Orig* videos and additionally 52 videos with permuted and missing steps, yielding 128 videos in total. We evaluate on both sets using pre-computed features provided by [34].

Evaluation Metrics. Following [56, 33, 34], we perform Hungarian matching between ground truth and predicted segments, which is conducted at the activity level. This is in contrast with the Hungarian matching performed at the video level in [1, 55, 15], which usually yields better results due to more fine-grained matching [65]. We compute Mean Over Frames (MOF), i.e., the percentage of frames with correct predictions averaged over all activities, and F1-Score, i.e., the harmonic mean of precision and recall, where only positive detections with more than 50% overlap with ground

	Method	MOF	F1
Eval	Frame	43.1	34.4
	Frame+Segment	<u>43.2</u>	<u>38.1</u>
	Frame+Segment+Alignment	55.8	50.3
YTI	Frame	42.8	30.2
	Frame+Segment	<u>45.0</u>	<u>30.8</u>
	Frame+Segment+Alignment	49.6	32.4

Table 1: Impacts of different model components on 50 Salads with the Eval granularity (*Eval*) and YouTube Instructions (*YTI*). Best results are in **bold**, while second best ones are underlined.

truth segments are considered. We compute F1-Score for each video and take the average over all videos.

4.1. Ablation Studies

4.1.1 Impacts of Different Model Components

We first study the effects of various network components on the 50 Salads (*Eval* granularity) and YTI datasets. The results are reported in Tab. 1. Firstly, using only the frame-level prediction module presented in Sec. 3.1 yields the lowest overall results. The frame-level prediction module exploits frame-level cues only and utilizes the fixed-order prior which does not account for permutations of actions. Next, we expand the network by adding the segment-level prediction module described in Sec. 3.2 to exploit segment-level cues. For 50 Salads, MOF is not changed much, while F1-score is improved by 3.7%. For YTI, MOF is increased by 2.2%, while F1-Score is slightly improved by 0.6%. Although the segment-level prediction module estimates the permutation-aware transcript, the framewise predictions are still suffered from over-segmentation. To address that, the frame-to-segment alignment module proposed in Sec. 3.3 is appended to the network to simultaneously leverage frame-level cues and segment-level cues and refine the framewise predictions, leading to significant performance gains. On 50 Salads, the results are boosted to 55.8% and 50.3% for MOF and F1-Score respectively, while on YTI, MOF is increased to 49.6% and F1-Score to 32.4%.

4.1.2 Impacts of Different Pseudo Labels

Here, we conduct an ablation study on the 50 Salads (*Eval* granularity) and YTI datasets by using various versions of pseudo labels Q_s and Q_a computed from either the fixed order of actions A or the permutation-aware transcript T . Tab. 2 presents the results. Firstly, using the fixed order of actions A for computing both Q_s and Q_a (i.e., we use $T = A$ in both Secs. 3.2 and 3.3) yields the lowest overall numbers on both datasets, i.e., on 50 Salads, 46.1% and 45.2% for MOF and F1-Score respectively, and

	Q_s	Q_a	MOF	F1
Eval	A	A	46.1	45.2
	T	A	50.8	46.9
	A	T	<u>54.0</u>	<u>48.7</u>
	T	T	55.8	50.3
YTI	A	A	44.3	29.4
	T	A	45.7	29.7
	A	T	<u>46.5</u>	<u>29.8</u>
	T	T	49.6	32.4

Table 2: Impacts of different pseudo labels on 50 Salads with the Eval granularity (*Eval*) and YouTube Instructions (*YTI*). Best results are in **bold**, while second best ones are underlined.

on YTI, 44.3% and 29.4% for MOF and F1-Score respectively. Next, we experiment with using the permutation-aware transcript T for computing either Q_s or Q_a , resulting in performance gains, e.g., for the former (T for Q_s , A for Q_a), we achieve 50.8% for MOF and 46.9% for F1-Score on 50 Salads, while for the latter (A for Q_s , T for Q_a), we obtain 54.0% for MOF and 48.7% for F1-Score on 50 Salads. Finally, we employ the permutation-aware transcript T for computing both Q_s and Q_a , leading to the best performance on both datasets, i.e., 55.8% for MOF and 50.3% for F1-Score on 50 Salads, and 49.6% for MOF and 32.4% for F1-Score on YTI. The above results confirm the benefits of using the permutation-aware transcript T for computing both pseudo labels Q_s and Q_a .

4.2. Comparisons with the State-of-the-Art

4.2.1 Results on 50 Salads

We now compare the MOF performance of our approach with state-of-the-art unsupervised activity segmentation methods on the 50 Salads dataset for both granularities, i.e., *Eval* and *Mid*. Tab. 3 illustrates the results. It is evident from Tab. 3 that our approach obtains the best numbers on both granularities, outperforming all competing methods. In particular, UFSA outperforms TOT [34] by 8.4% and 4.9% on the *Eval* and *Mid* granularities respectively, and UDE [61] by 13.6% on the *Eval* granularity. Although TOT [34] and UDE [61] conduct joint representation learning and online clustering as our approach, they only exploit frame-level cues, whereas UFSA leverages segment-level cues as well. Moreover, our approach achieves better results than SSCAP [68], which uses recent self-supervised learning features [16], and ASAL [42], which exploits segment-level cues via action shuffling, e.g., on the *Eval* granularity, UFSA achieves 55.8% MOF, whereas SSCAP [68] and ASAL [42] obtain 41.4% MOF and 39.2% MOF respectively. The substantial improvements of UFSA over previous methods demonstrate the effectiveness of our approach.

Method	Eval	Mid
CTE [33]	35.5	30.2
VTE [65]	30.6	24.2
ASAL [42]	39.2	<u>34.4</u>
UDE [61]	42.2	-
SSCAP [68]	41.4	-
TOT [34]	<u>47.4</u>	31.8
Ours (UFSA)	55.8	36.7

Table 3: Results on 50 Salads. *Eval* denotes the Eval granularity, while *Mid* denotes the Mid granularity. Best results are in **bold**, while second best ones are underlined.

Method	MOF	F1
Frank-Wolfe [3]	-	24.4
Mallow [56]	27.8	27.0
CTE [33]	39.0	28.3
VTE [65]	-	29.9
ASAL [42]	<u>44.9</u>	<u>32.1</u>
UDE [61]	43.8	29.6
TOT [34]	40.6	30.0
Ours (UFSA)	49.6	32.4

Table 4: Results on YouTube Instructions. Best results are in **bold**, while second best ones are underlined.

4.2.2 Results on YouTube Instructions

Tab. 4 presents the quantitative results of our approach along with previous unsupervised activity segmentation methods on the YTI dataset. We follow the protocol of prior works and report the accuracy excluding the background frames. It is clear from Tab. 4 that our approach achieves the best results on both metrics, outperforming all previous methods. Specifically, UFSA has an improvement of 9.0% MOF and 2.4% F1-Score over TOT [34], and an improvement of 5.8% MOF and 2.8% F1-Score over UDE [61]. In addition, our approach obtains a noticeable gain of 4.7% MOF and a slight gain of 0.3% F1-Score over ASAL [42]. Fig. 6 plots the qualitative results of UFSA, TOT [34], and CTE [33] on a YTI video. Our approach demonstrates significant advantages over CTE [33] and TOT [34] in terms of capturing the temporal order of actions and aligning them closely with the ground truth. Please refer to the supplementary material for more qualitative results.

4.2.3 Results on Breakfast

Tab. 5 includes the performance of different methods on the Breakfast dataset. From Tab. 5, our results are on par with ASAL [42], which leverages segment-level informa-

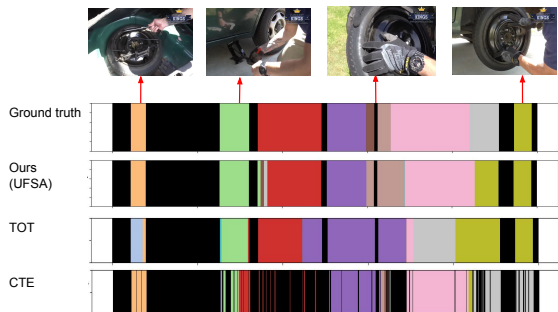


Figure 6: Segmentation results on a YouTube Instructions video. Black color indicates background frames.

Method	MOF	F1
Mallow [56]	34.6	-
CTE [33]	41.8	26.4
VTE [65]	48.1	-
ASAL [42]	52.5	37.9
UDE [61]	47.4	31.9
SSCAP [68]	51.1	39.2
TOT [34]	47.5	31.0
Ours (UFSA)	<u>52.1</u>	<u>38.0</u>

Table 5: Results on Breakfast. Best results are in **bold**, while second best ones are underlined.

tion via action shuffling, and SSCAP [68], which employs more sophisticated self-supervised features [16]. Particularly, ASAL [42] and SSCAP [68] yield the best MOF number (i.e., 52.5%) and the best F1-Score number (i.e., 39.2%) respectively, while UFSA achieves the second best results for both metrics (i.e., 52.1% and 38.0%). In addition, our approach outperforms a number of competing methods, namely Mallow [56], CTE [33], VTE [65], UDE [61], and TOT [34], which exploit frame-level cues only.

4.2.4 Results on Desktop Assembly

Here, we compare the performance of our approach with CTE [33] and TOT [34] on the Desktop Assembly dataset for both sets, i.e., *Orig* and *Extra*. The results are reported in Tab. 6, which shows superior performance of our approach over CTE [33] and TOT [34]. For example, UFSA achieves an improvement of 14.9% MOF and 20.5% F1-Score over TOT [34] on the *Orig* set, and an improvement of 7.6% MOF and 15.5% F1-Score over TOT [34] on the *Extra* set. The results on the *Orig* set indicate the effectiveness of our approach in preserving the fixed order of actions, while the results on the *Extra* set show the ability of our method in handling permutations of actions.

	Method	MOF	F1
Orig	CTE [33]	47.6	44.9
	TOT [34]	<u>56.3</u>	<u>51.7</u>
	Ours (UFSA)	71.2	72.2
Extra	CTE [33]	40.8	35.6
	TOT [34]	<u>51.0</u>	<u>40.4</u>
	Ours (UFSA)	58.6	55.9

Table 6: Results on Desktop Assembly. *Orig* includes original fixed-order videos only, while *Extra* further includes additional permuted-step and missing-step videos. Best results are in **bold**, while second best ones are underlined.

	Method	MOF	F1
Eval	CTE [33]	28.6	26.4
	TOT [34]	<u>39.8</u>	<u>37.0</u>
	Ours (UFSA)	47.6	41.8
YTI	CTE [33]	38.4	25.5
	TOT [34]	<u>40.4</u>	<u>28.0</u>
	Ours (UFSA)	46.8	28.2
Breakfast	CTE [33]	39.8	25.5
	TOT [34]	<u>40.6</u>	<u>27.6</u>
	Ours (UFSA)	44.0	36.7
Orig	CTE [33]	35.6	31.8
	TOT [34]	<u>55.3</u>	<u>50.2</u>
	Ours (UFSA)	63.9	63.7
Extra	CTE [33]	35.7	30.4
	TOT [34]	<u>43.6</u>	<u>35.0</u>
	Ours (UFSA)	57.9	54.0

Table 7: Generalization results. Best results are in **bold**, while second best ones are underlined.

4.2.5 Generalization Results

We follow [34] to evaluate the generalization ability of our approach. We divide the datasets, i.e., 50 Salads (*Eval* granularity), YTI, Breakfast, Desktop Assembly (*Orig* and *Extra* sets) into 80% for training and 20% for testing. We compare our approach with CTE [33] and TOT [34]. The results are shown in Tab. 7. It can be seen from Tab. 7 that UFSA continues to outperform CTE [33] and TOT [34] in this experiment setting. Note the results of CTE [33] and TOT [34] in Tab. 7 are different from those reported in [34] due to different splits. We will make our splits publicly available.

5. Conclusion

We propose a novel combination of modules and losses to exploit both frame-level cues and segment-level cues for unsupervised activity segmentation. Our approach includes a frame-level prediction module which uses a transformer encoder for obtaining framewise action classes and

is trained in unsupervised manner. To leverage segment-level cues, we add a segment-level prediction model based on a transformer encoder for predicting video transcripts and a frame-to-segment alignment module for corresponding frame-level features with segment-level features, resulting in permutation-aware segmentation results. Moreover, we present simple-yet-effective pseudo labels for unsupervised training of the above modules. We show comparable or superior results of our approach over prior unsupervised activity segmentation methods on 50 Salads, YouTube Instructions, Breakfast, and Desktop Assembly. Our future work will explore handling repetitive actions [67] or other techniques [8, 20, 46, 63] for frame-to-segment alignment.

A. Supplementary Material

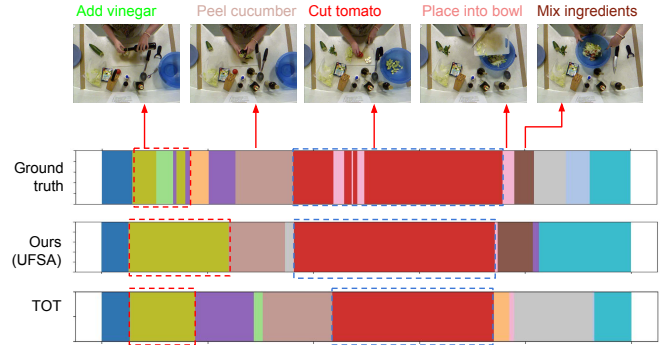
This supplementary material begins with some qualitative results in Sec. A.1. We then provide the details of our implementation in Sec. A.2. Finally, Sec. A.3 includes a discussion on the societal impacts of our work.

A.1. Qualitative Results

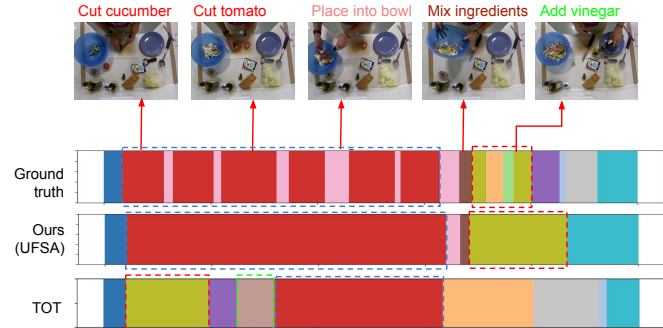
Fig. 7 illustrates the segmentation results of our approach and TOT [34] on two 50 Salads videos (*Eval* granularity). From Fig. 7, UFSA shows superior performance in extracting the permutation of actions. For example, let us consider the ‘Add vinegar’ action (highlighted by red boxes) which happens at different temporal positions in the videos, UFSA captures the permutation of actions correctly, while TOT [34] maintains the fixed order of actions and hence fails to recognize the permutation of actions. Next, for actions that are missing, such as the ‘Peel cucumber’ action, which occurs in Fig. 7a but does not appear in Fig. 7b, UFSA associates a negligible number of frames with this action class, whereas TOT [34] incorrectly assigns a large number of frames (highlighted by a green box).

Moreover, we include in Fig. 8 the segmentation results of our approach, TOT [34], and CTE [33] on other datasets, namely YouTube Instructions, Breakfast, and Desktop Assembly (*Orig* set). It is evident from Fig. 8 that our segmentation results are consistently closer to the ground truth than those of TOT [34] and CTE [33].

Nevertheless, our approach has a limitation in handling repetitive actions. For example, let us look at the ‘Cut’ action in Fig. 7, which includes ‘Cut tomato’, ‘Cut cucumber’, ‘Cut cheese’, and ‘Cut lettuce’ and hence occurs multiple times in the videos, our approach merges the multiple occurrences into a large segment (highlighted by blue boxes) since it assumes each action can happen only once. In addition, although TOT [34] has the same drawback, our combined segments are closer to the ground truth. Our future work will investigate handling repetitive actions.



(a) 50 Salads (*rgb-21-01*).



(b) 50 Salads (*rgb-15-02*).

Figure 7: Segmentation results on two 50 Salads videos (*Eval* granularity). Red boxes highlight permuted actions. Green boxes highlight missing actions. Blue boxes highlight repetitive actions.

A.2. Implementation Details

Hyperparameter Settings. Tab. 8 presents a summary of our hyperparameter settings. For the temporal optimal transport problem in our frame-level prediction module and frame-to-segment alignment module, we follow the same hyperparameter settings used in TOT [34], including ρ and number of Sinkhorn-Knopp iterations. We keep the feature dimension d the same as TOT [34]. We use a single video, including all frames, per batch. In addition, for our transformer encoder and transformer decoder, we follow the same hyperparameter settings used in UVAST [5], including encoder dropout ratio and decoder dropout ratio. We set the temperature $\tau = 0.1$ (same as TOT [34]) in Sec. 3.1 of the main paper and the temperature $\tau' = 10^{-3}$ (same as UVAST [5]) in Sec. 3.3 of the main paper.

Computing Resources. All of our experiments are conducted with a single Nvidia A100 SXM4 GPU on Lambda Cloud.

Hyperparameter	Value
Temperature (τ)	0.1
Rho (ρ)	0.07 (E), 0.08 (M), 0.08 (Y), 0.05 (B), 0.07 (O), 0.07 (A)
Number of Sinkhorn-Knopp iterations	3
Feature dimension (d)	30 (E), 30 (M), 200 (Y), 40 (B), 30 (O), 30 (A)
Batch size	1
Learning rate	10^{-3}
Weight decay	10^{-5}
Number of encoder layers	2
Number of decoder layers	2
Encoder dropout ratio	0.3
Decoder dropout ratio	0.1
Temperature (τ')	10^{-3}

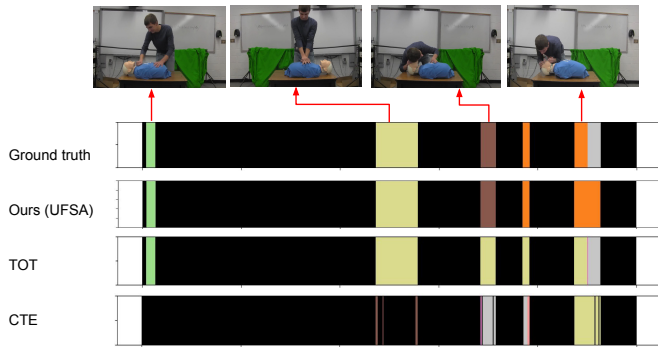
Table 8: Hyperparameter settings. **E** denotes 50 Salads (*Eval* granularity), **M** denotes 50 Salads (*Mid* granularity), **Y** denotes YouTube Instructions, **B** denotes Breakfast, **O** denotes Desktop Assembly (*Orig* set), and **A** denotes Desktop Assembly (*Extra* set).

A.3. Societal Impacts

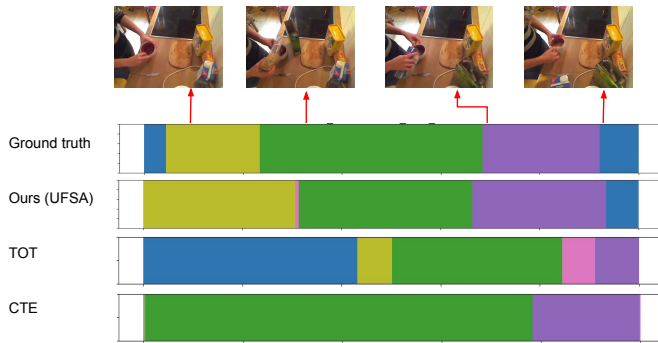
Our approach facilitates video recognition model learning without action labels, with potential applications in frontline worker training and assistance. Models generated from expert demonstration videos in various domains could offer guidance to new workers, improving the standard of care in fields such as medical surgery. However, at the same time, video understanding algorithms in surveillance applications may compromise privacy, even if it enhances security and productivity. Thus, we urge caution in the implementation of such technologies and advocate for the development of appropriate ethical guidelines.

References

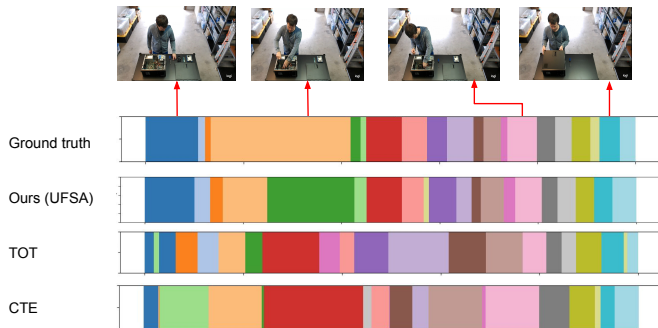
- [1] Sathyanarayanan N Aakur and Sudeep Sarkar. A perceptual prediction framework for self supervised event segmentation. In *Proceedings of the IEEE/CVF Conference on Computer Vision and Pattern Recognition*, pages 1197–1206, 2019. 6
- [2] Oguz Akkas, Cheng Hsien Lee, Yu Hen Hu, Carisa Harris Adamson, David Rempel, and Robert G Radwin. Measuring exertion time, duty cycle and hand activity level for industrial tasks using computer vision. *Ergonomics*, 60(12):1730–1738, 2017. 1
- [3] Jean-Baptiste Alayrac, Piotr Bojanowski, Nishant Agrawal, Josef Sivic, Ivan Laptev, and Simon Lacoste-Julien. Unsupervised learning from narrated instruction videos. In *Proceedings of the IEEE Conference on Computer Vision and Pattern Recognition*, pages 4575–4583, 2016. 2, 6, 7
- [4] Anurag Arnab, Mostafa Dehghani, Georg Heigold, Chen Sun, Mario Lučić, and Cordelia Schmid. Vivit: A video vision transformer. In *Proceedings of the IEEE/CVF international conference on computer vision*, pages 6836–6846, 2021. 3
- [5] Nadine Behrmann, S Alireza Golestaneh, Zico Kolter, Jürgen Gall, and Mehdi Noroozi. Unified fully and timestamp supervised temporal action segmentation via sequence to sequence translation. In *European Conference on Computer Vision*, pages 52–68. Springer, 2022. 1, 2, 3, 5, 6, 9
- [6] Gedas Bertasius, Heng Wang, and Lorenzo Torresani. Is space-time attention all you need for video understanding? In *ICML*, volume 2, page 4, 2021. 3
- [7] Jonas Blattgerste, Benjamin Streng, Patrick Renner, Thies Pfeiffer, and Kai Essig. Comparing conventional and augmented reality instructions for manual assembly tasks. In *Proceedings of the 10th international conference on pervasive technologies related to assistive environments*, pages 75–82, 2017. 1
- [8] Chien-Yi Chang, De-An Huang, Yanan Sui, Li Fei-Fei, and Juan Carlos Niebles. D3tw: Discriminative differentiable dynamic time warping for weakly supervised action alignment and segmentation. In *Proceedings of the IEEE/CVF Conference on Computer Vision and Pattern Recognition*, pages 3546–3555, 2019. 1, 2, 9
- [9] Chun-Fu Richard Chen, Quanfu Fan, and Rameswar Panda. Crossvit: Cross-attention multi-scale vision transformer for image classification. In *Proceedings of the IEEE/CVF international conference on computer vision*, pages 357–366, 2021. 3
- [10] Marco Cuturi. Sinkhorn distances: Lightspeed computation of optimal transport. *Advances in neural information processing systems*, 26:2292–2300, 2013. 3, 5
- [11] Guodong Ding, Fadime Sener, and Angela Yao. Temporal action segmentation: An analysis of modern technique. *arXiv preprint*, 2022. 1
- [12] Li Ding and Chenliang Xu. Tricorner: A hybrid temporal convolutional and recurrent network for video action segmentation. *arXiv preprint*, 2017. 1, 2
- [13] Li Ding and Chenliang Xu. Weakly-supervised action segmentation with iterative soft boundary assignment. In *Pro-*



(a) YouTube Instructions (*cpr_0027*).



(b) Breakfast (*P13_webcam01_P13_cereals*).



(c) Desktop Assembly (*2020-04-19_17-24-35*).

Figure 8: Segmentation results on (a) a YouTube Instructions video, (b) a Breakfast video, and (c) a Desktop Assembly video (‘Orig’ set).

ceedings of the IEEE Conference on Computer Vision and Pattern Recognition, pages 6508–6516, 2018. 1, 2

- [14] Alexey Dosovitskiy, Lucas Beyer, Alexander Kolesnikov, Dirk Weissenborn, Xiaohua Zhai, Thomas Unterthiner, Mostafa Dehghani, Matthias Minderer, Georg Heigold, Sylvain Gelly, et al. An image is worth 16x16 words: Transformers for image recognition at scale. In *International Conference on Learning Representations*. 2, 3
- [15] Zexing Du, Xue Wang, Guoqing Zhou, and Qing Wang. Fast

and unsupervised action boundary detection for action segmentation. In *Proceedings of the IEEE/CVF Conference on Computer Vision and Pattern Recognition*, pages 3323–3332, 2022. 6

- [16] Dave Epstein, Boyuan Chen, and Carl Vondrick. Oops! predicting unintentional action in video. In *Proceedings of the IEEE/CVF conference on computer vision and pattern recognition*, pages 919–929, 2020. 7, 8
- [17] Yazan Abu Farha and Jurgen Gall. Ms-tcn: Multi-stage temporal convolutional network for action segmentation. In *Proceedings of the IEEE/CVF conference on computer vision and pattern recognition*, pages 3575–3584, 2019. 1, 2
- [18] Mohsen Fayyaz and Jurgen Gall. Sct: Set constrained temporal transformer for set supervised action segmentation. In *Proceedings of the IEEE/CVF Conference on Computer Vision and Pattern Recognition*, pages 501–510, 2020. 2
- [19] Markus Funk, Thomas Kosch, Scott W Greenwald, and Albrecht Schmidt. A benchmark for interactive augmented reality instructions for assembly tasks. In *Proceedings of the 14th international conference on mobile and ubiquitous multimedia*, pages 253–257, 2015. 1
- [20] Sanjay Haresh, Sateesh Kumar, Huseyin Coskun, Shahram N Syed, Andrey Konin, Zeeshan Zia, and Quoc-Huy Tran. Learning by aligning videos in time. In *Proceedings of the IEEE/CVF Conference on Computer Vision and Pattern Recognition*, pages 5548–5558, 2021. 9
- [21] Sanjay Haresh, Sateesh Kumar, M Zeeshan Zia, and Quoc-Huy Tran. Towards anomaly detection in dashcam videos. In *2020 IEEE Intelligent Vehicles Symposium (IV)*, pages 1407–1414. IEEE, 2020. 1
- [22] Yifei Huang, Yusuke Sugano, and Yoichi Sato. Improving action segmentation via graph-based temporal reasoning. In *Proceedings of the IEEE/CVF conference on computer vision and pattern recognition*, pages 14024–14034, 2020. 2
- [23] Yuchi Ishikawa, Seito Kasai, Yoshimitsu Aoki, and Hirokatsu Kataoka. Alleviating over-segmentation errors by detecting action boundaries. In *Proceedings of the IEEE/CVF winter conference on applications of computer vision*, pages 2322–2331, 2021. 2
- [24] Jirasak Ji, Warut Pannakkong, and Jirachai Buddhakulsomsiri. A computer vision-based model for automatic motion time study. *CMC-COMPUTERS MATERIALS & CON-TINUA*, 73(2):3557–3574, 2022. 1
- [25] Jirasak Ji, Warut Pannakkong, Pham Duc Tai, Chawalit Jeenanunta, and Jirachai Buddhakulsomsiri. Motion time study with convolutional neural network. In *Integrated Uncertainty in Knowledge Modelling and Decision Making: 8th International Symposium, IUKM 2020, Phuket, Thailand, November 11–13, 2020, Proceedings 8*, pages 249–258. Springer, 2020. 1
- [26] Svebor Karaman, Lorenzo Seidenari, and Alberto Del Bimbo. Fast saliency based pooling of fisher encoded dense trajectories. In *ECCV THUMOS Workshop*, volume 1, page 5, 2014. 2
- [27] Hamza Khan, Sanjay Haresh, Awais Ahmed, Shakeeb Siddiqui, Andrey Konin, M Zeeshan Zia, and Quoc-Huy Tran. Timestamp-supervised action segmentation with graph con-

- volutional networks. In *2022 IEEE/RSJ International Conference on Intelligent Robots and Systems (IROS)*, pages 10619–10626. IEEE, 2022. [1](#), [2](#)
- [28] Diederik P Kingma and Jimmy Ba. Adam: A method for stochastic optimization. *arXiv preprint*, 2014. [6](#)
- [29] Andrey Konin, Shakeeb Siddiqui, Hasan Gilani, Muhammad Mudassir, M Hassan Ahmed, Taban Shaukat, Muhammad Naufil, Awais Ahmed, Quoc-Huy Tran, and M Zeeshan Zia. Ai-mediated job status tracking in ar as a no-code service. In *2022 IEEE International Symposium on Mixed and Augmented Reality Adjunct (ISMAR-Adjunct)*, pages 1–2. IEEE, 2022. [1](#)
- [30] Hilde Kuehne, Ali Arslan, and Thomas Serre. The language of actions: Recovering the syntax and semantics of goal-directed human activities. In *Proceedings of the IEEE conference on computer vision and pattern recognition*, pages 780–787, 2014. [6](#)
- [31] Hilde Kuehne, Juergen Gall, and Thomas Serre. An end-to-end generative framework for video segmentation and recognition. In *2016 IEEE Winter Conference on Applications of Computer Vision (WACV)*, pages 1–8. IEEE, 2016. [2](#), [6](#)
- [32] Hilde Kuehne, Alexander Richard, and Juergen Gall. Weakly supervised learning of actions from transcripts. *Computer Vision and Image Understanding*, 163:78–89, 2017. [1](#), [2](#)
- [33] Anna Kukleva, Hilde Kuehne, Fadime Sener, and Jurgen Gall. Unsupervised learning of action classes with continuous temporal embedding. In *Proceedings of the IEEE/CVF Conference on Computer Vision and Pattern Recognition*, pages 12066–12074, 2019. [1](#), [2](#), [6](#), [7](#), [8](#), [9](#)
- [34] Sateesh Kumar, Sanjay Hareesh, Awais Ahmed, Andrey Konin, M Zeeshan Zia, and Quoc-Huy Tran. Unsupervised action segmentation by joint representation learning and on-line clustering. In *Proceedings of the IEEE/CVF Conference on Computer Vision and Pattern Recognition*, pages 20174–20185, 2022. [1](#), [2](#), [3](#), [5](#), [6](#), [7](#), [8](#), [9](#)
- [35] Colin Lea, Michael D Flynn, Rene Vidal, Austin Reiter, and Gregory D Hager. Temporal convolutional networks for action segmentation and detection. In *proceedings of the IEEE Conference on Computer Vision and Pattern Recognition*, pages 156–165, 2017. [1](#), [2](#)
- [36] Chen-Yu Lee, Saining Xie, Patrick Gallagher, Zhengyou Zhang, and Zhuowen Tu. Deeply-supervised nets. In *Artificial intelligence and statistics*, pages 562–570. PMLR, 2015. [5](#)
- [37] Peng Lei and Sinisa Todorovic. Temporal deformable residual networks for action segmentation in videos. In *Proceedings of the IEEE conference on computer vision and pattern recognition*, pages 6742–6751, 2018. [1](#), [2](#)
- [38] Chi Li, M Zeeshan Zia, Quoc-Huy Tran, Xiang Yu, Gregory D Hager, and Manmohan Chandraker. Deep supervision with shape concepts for occlusion-aware 3d object parsing. In *Proceedings of the IEEE conference on computer vision and pattern recognition*, pages 5465–5474, 2017. [5](#)
- [39] Chi Li, M Zeeshan Zia, Quoc-Huy Tran, Xiang Yu, Gregory D Hager, and Manmohan Chandraker. Deep supervision with intermediate concepts. *IEEE transactions on pattern analysis and machine intelligence*, 41(8):1828–1843, 2018. [5](#)
- [40] Jun Li, Peng Lei, and Sinisa Todorovic. Weakly supervised energy-based learning for action segmentation. In *Proceedings of the IEEE/CVF International Conference on Computer Vision*, pages 6243–6251, 2019. [1](#), [2](#)
- [41] Jun Li and Sinisa Todorovic. Set-constrained viterbi for set-supervised action segmentation. In *Proceedings of the IEEE/CVF Conference on Computer Vision and Pattern Recognition*, pages 10820–10829, 2020. [2](#)
- [42] Jun Li and Sinisa Todorovic. Action shuffle alternating learning for unsupervised action segmentation. In *Proceedings of the IEEE/CVF Conference on Computer Vision and Pattern Recognition*, pages 12628–12636, 2021. [2](#), [6](#), [7](#), [8](#)
- [43] Shi-Jie Li, Yazan AbuFarha, Yun Liu, Ming-Ming Cheng, and Juergen Gall. Ms-tcn++: Multi-stage temporal convolutional network for action segmentation. *IEEE Transactions on Pattern Analysis and Machine Intelligence*, 2020. [1](#), [2](#)
- [44] Zhe Li, Yazan Abu Farha, and Jurgen Gall. Temporal action segmentation from timestamp supervision. In *Proceedings of the IEEE/CVF Conference on Computer Vision and Pattern Recognition*, pages 8365–8374, 2021. [1](#), [2](#)
- [45] Lai Xing Ng, Jamie Ng, Keith TW Tang, Liyuan Li, Mark Rice, and Marcus Wan. Using visual intelligence to automate maintenance task guidance and monitoring on a head-mounted display. In *Proceedings of the 2019 5th International Conference on Robotics and Artificial Intelligence*, pages 70–75, 2019. [1](#)
- [46] Khoi D Nguyen, Quoc-Huy Tran, Khoi Nguyen, Binh-Son Hua, and Rang Nguyen. Inductive and transductive few-shot video classification via appearance and temporal alignments. In *Computer Vision—ECCV 2022: 17th European Conference, Tel Aviv, Israel, October 23–27, 2022, Proceedings, Part XX*, pages 471–487. Springer, 2022. [9](#)
- [47] Behnoosh Parsa and Ashis G Banerjee. A multi-task learning approach for human activity segmentation and ergonomics risk assessment. In *Proceedings of the IEEE/CVF Winter Conference on Applications of Computer Vision*, pages 2352–2362, 2021. [1](#)
- [48] Behnoosh Parsa, Behzad Dariush, et al. Spatio-temporal pyramid graph convolutions for human action recognition and postural assessment. In *Proceedings of the IEEE/CVF Winter Conference on Applications of Computer Vision*, pages 1080–1090, 2020. [1](#)
- [49] Adam Paszke, Sam Gross, Soumith Chintala, Gregory Chanan, Edward Yang, Zachary DeVito, Zeming Lin, Alban Desmaison, Luca Antiga, and Adam Lerer. Automatic differentiation in pytorch. 2017. [6](#)
- [50] Rahul Rahaman, Dipika Singhania, Alexandre Thiery, and Angela Yao. A generalized and robust framework for timestamp supervision in temporal action segmentation. In *Computer Vision—ECCV 2022: 17th European Conference, Tel Aviv, Israel, October 23–27, 2022, Proceedings, Part IV*, pages 279–296. Springer, 2022. [1](#), [2](#)
- [51] Alexander Richard, Hilde Kuehne, and Juergen Gall. Weakly supervised action learning with rnn based fine-to-coarse modeling. In *Proceedings of the IEEE Conference on Computer Vision and Pattern Recognition*, pages 754–763, 2017. [1](#), [2](#)

- [52] Alexander Richard, Hilde Kuehne, and Juergen Gall. Action sets: Weakly supervised action segmentation without ordering constraints. In *Proceedings of the IEEE conference on Computer Vision and Pattern Recognition*, pages 5987–5996, 2018. [2](#)
- [53] Alexander Richard, Hilde Kuehne, Ahsan Iqbal, and Juergen Gall. Neuralnetwork-viterbi: A framework for weakly supervised video learning. In *Proceedings of the IEEE Conference on Computer Vision and Pattern Recognition*, pages 7386–7395, 2018. [1](#), [2](#)
- [54] Marcus Rohrbach, Sikandar Amin, Mykhaylo Andriluka, and Bernt Schiele. A database for fine grained activity detection of cooking activities. In *2012 IEEE conference on computer vision and pattern recognition*, pages 1194–1201. IEEE, 2012. [2](#)
- [55] Saquib Sarfraz, Naila Murray, Vivek Sharma, Ali Diba, Luc Van Gool, and Rainer Stiefelhagen. Temporally-weighted hierarchical clustering for unsupervised action segmentation. In *Proceedings of the IEEE/CVF Conference on Computer Vision and Pattern Recognition*, pages 11225–11234, 2021. [6](#)
- [56] Fadime Sener and Angela Yao. Unsupervised learning and segmentation of complex activities from video. In *Proceedings of the IEEE Conference on Computer Vision and Pattern Recognition*, pages 8368–8376, 2018. [2](#), [6](#), [7](#), [8](#)
- [57] Ozan Sener, Amir R Zamir, Silvio Savarese, and Ashutosh Saxena. Unsupervised semantic parsing of video collections. In *Proceedings of the IEEE International Conference on Computer Vision*, pages 4480–4488, 2015. [2](#)
- [58] Yaser Souri, Yazan Abu Farha, Emad Bahrami, Gianpiero Francesca, and Juergen Gall. Robust action segmentation from timestamp supervision. *arXiv preprint*, 2022. [1](#), [2](#)
- [59] Sebastian Stein and Stephen J McKenna. Combining embedded accelerometers with computer vision for recognizing food preparation activities. In *Proceedings of the 2013 ACM international joint conference on Pervasive and ubiquitous computing*, pages 729–738, 2013. [6](#)
- [60] Bing Su and Gang Hua. Order-preserving wasserstein distance for sequence matching. In *Proceedings of the IEEE conference on computer vision and pattern recognition*, pages 1049–1057, 2017. [3](#)
- [61] Sirnam Swetha, Hilde Kuehne, Yogesh S Rawat, and Mubarak Shah. Unsupervised discriminative embedding for sub-action learning in complex activities. In *2021 IEEE International Conference on Image Processing (ICIP)*, pages 2588–2592. IEEE, 2021. [1](#), [2](#), [6](#), [7](#), [8](#)
- [62] Kevin Tang, Li Fei-Fei, and Daphne Koller. Learning latent temporal structure for complex event detection. In *2012 IEEE Conference on Computer Vision and Pattern Recognition*, pages 1250–1257. IEEE, 2012. [2](#)
- [63] Quoc-Huy Tran, Muhammad Ahmed, Ahmed Mehmood, M Hassan Ahmed, Murad Popattia, Andrey Konin, and M Zeeshan Zia. Learning by aligning 2d skeleton sequences in time. *arXiv preprint*, 2023. [9](#)
- [64] Ashish Vaswani, Noam Shazeer, Niki Parmar, Jakob Uszkoreit, Llion Jones, Aidan N Gomez, Łukasz Kaiser, and Illia Polosukhin. Attention is all you need. *Advances in neural information processing systems*, 30, 2017. [2](#), [3](#)
- [65] Rosaura G VidalMata, Walter J Scheirer, Anna Kukleva, David Cox, and Hilde Kuehne. Joint visual-temporal embedding for unsupervised learning of actions in untrimmed sequences. In *Proceedings of the IEEE/CVF Winter Conference on Applications of Computer Vision*, pages 1238–1247, 2021. [2](#), [6](#), [7](#), [8](#)
- [66] Heng Wang and Cordelia Schmid. Action recognition with improved trajectories. In *Proceedings of the IEEE international conference on computer vision*, pages 3551–3558, 2013. [6](#)
- [67] Qifei Wang, Gregorij Kurillo, Ferda Ofli, and Ruzena Bajcsy. Unsupervised temporal segmentation of repetitive human actions based on kinematic modeling and frequency analysis. In *2015 international conference on 3D vision*, pages 562–570. IEEE, 2015. [9](#)
- [68] Zhe Wang, Hao Chen, Xinyu Li, Chunhui Liu, Yuanjun Xiong, Joseph Tighe, and Charless Fowlkes. Sscap: Self-supervised co-occurrence action parsing for unsupervised temporal action segmentation. In *Proceedings of the IEEE/CVF Winter Conference on Applications of Computer Vision*, pages 1819–1828, 2022. [2](#), [6](#), [7](#), [8](#)
- [69] Fangqiu Yi, Hongyu Wen, and Tingting Jiang. Asformer: Transformer for action segmentation. *arXiv preprint*, 2021. [3](#)